NURETH14-77

PROPERTIES OF FLOODING WAVES IN VERTICAL CHURN FLOW

Ke Wang, Bofeng Bai, Bo Yang and Chen Xie

State Key Laboratory of Multiphase Flow in Power Engineering, Xi'an Jiaotong University, Shaanxi, China

Abstract

It is more accurate to predict the critical heat flux (CHF) from the start of churn flow rather than the start of annular flow. High-speed photography has been employed for qualitative investigation of entrainment in vertical two-phase flow under churn flow condition. This paper mainly focuses on the evolution of the flooding waves close to the water inlet section and liquid distribution in the cross-section of tube. The properties of flooding wave such as frequency and amplitude have been obtained.

1. Introduction

The critical heat flux (CHF) is one of the most important factors for the system security of engineering applications, such as nuclear reactors, power plants and boilers. In annular flow, excessive liquid entrainment could lead to "dry out" conditions in which the liquid film is completely depleted from the pipe walls. This heat transfer deterioration would then cause the pipe superheated even explosion. Therefore, an accurate prediction is especially important to prevent such conditions.

Recently, Ahmad et al. [1] put forward that it is more reasonable for dryout model to start integration of entrainment and deposition processes from the start of churn flow rather than the annular flow. Furthermore, interfacial waves have been identified as the major source of entrained droplets in liquid-gas flow. Therefore, knowledge of wave properties in churn flow is essential for the development of mechanistic models for the prediction dryout condition.

Churn flow normally occurs in vertical or near vertical upward flow. However, the relative researches on churn flow available in literature still lack due to its complexity, even its definition still has controversy. Zuber and Findley [2] took churn flow as a type of bubble flow, while Taitel et al. [3] considered it as a developing slug flow. Hewitt and Hall Taylor [4] proposed that churn flow is an intermediate flow regime between slug and annular flow, and occurs after the break down of slug flow when velocity increases. Jayanti and Hewitt [5] investigated four models for slug-churn flow transitions (entrance effect mechanism, flooding mechanism, wake effect mechanism and bubble coalescence mechanism) and pointed out that the flooding mechanism is more proper to interpret this transition. In addition, Jayanti et al. [6] made an observation and confirmed that flooding waves appear within the Taylor bubbles as the transition is approached. Owen [7] proposed that there is a sudden increase in pressure gradient at the breakdown of slug flow and the formation of churn flow. After that, the pressure gradient decreases when increasing the air flow rate, eventually increasing again when entering the annular flow region. Therefore, the definition of churn flow as an intermediate flow regime is adopted in this paper.

The 14th International Topical Meeting on Nuclear Reactor Thermalhydraulics, NURETH-14 Toronto, Ontario, Canada, September 25-30, 2011

Churn flow has similarities to annular flow, e.g. a continuous gas core in the centre of the pipe and a liquid film near the wall. But the most relevant feature that distinguishes churn flow from annular flow is the existence of flooding waves travelling upwards over a falling film throughout the regime like in Taylor bubbles in slug flow. As gas velocity increases, the liquid downward film ultimately ceases and gives rise to a unidirectional annular flow. This flow reversal point is reached when the dimensionless superficial gas velocity U_{sg}^* approximates unity (Hewitt et al. [8]; Wallis [9]). The dimensionless superficial gas velocity is defined as:

$$U_{sg}^* = u_{sg} \sqrt{\frac{\rho_G}{gd(\rho_L - \rho_G)}} \approx 1$$
 (1)

Where u_{sg} , d, ρ_L , ρ_G are the gas superficial velocity, diameter of tube, liquid density and air density, respectively.

Unlike annular flow, the entrained fraction in churn flow decreases with increasing gas superficial velocity. When passes through a minimum around the transition, entrained fraction increases again in annular flow. This has been verified by experiments of Verbeek et al. [10], Azzopardi and Zaidi [11], Barbosa et al. [12], Wallis et al. [13] and Azzopardi and Wren [14]. Generally, the mechanism of entrainment in churn flow is supposed as undercut or bag break-up proposed by Azzopardi [15]. And the drop deposition in churn flow is often dominated by radial velocities imparted at the point of droplet creation.

However, it is hard to investigate the properties in actual transition region. Therefore, an "analogous churn" flow is introduced. Govan et al. [16] compared the pressure gradient and hold-up in the region above the liquid injector both with and without the falling liquid film below the injector. They proved that no significant difference exists between the two cases. Thus, the transition to churn flow is characterized by the capability of forming flooding-type waves and there is an intimate connection between the flooding phenomenon and the existence of churn flow. Based on these conclusions, Barbosa et al. [17] carried out their experimental and modelling work on an "analogous churn" flow in a vertical pipe. They showed the process of the wave formation and motion in a 31.8 mm i.d. tube using high-speed video recordings over a churn flow condition. They also proposed a mathematical model for wave levitation process which takes into account forces acting on a circumferentially coherent wave. Subsequently, Enrico and Davide [18] simulated the churn flow regime of air-water and R134a vapour-liquid mixtures in vertical pipe by means of VOF method, and made a comparison with experiment data. They also proposed a simplified model of the levitation process of the ring-type waves typical in churn flow at different liquid and gas superficial velocities and pipe diameters.

This paper mainly focuses on the evolution of the flooding waves close to the water inlet section and liquid distribution in the cross-section of tube. High-speed photography has been employed for qualitative investigation of properties of flooding wave and mechanism of entrainment in vertical two-phase flow over churn flow condition. Since the film oscillates in flow direction, the conventional method for measurement of entrained fraction (extracting the liquid film) is not feasible in this pattern. Therefore, liquid distribution in the cross-section of tube is still measured using optical method.

2. Experimental System and Method

2.1 Experimental System

The experimental system, as seen in Figure 1, consists of a gas loop, a water loop and a test section. The air from the compressor flows through the regulator valve and is separated into two ways: one part of developed gas is fed into the test section at the bottom of the tube; the other flows into the branch gas channel, respectively. The water is pumped into the test section using a 0.55 kW pump through porous wall. It can be observed that the water can be removed from the test section through two ways: the upward film would be removed from the upper outlet and the falling film could be extracted from the extraction sinter.

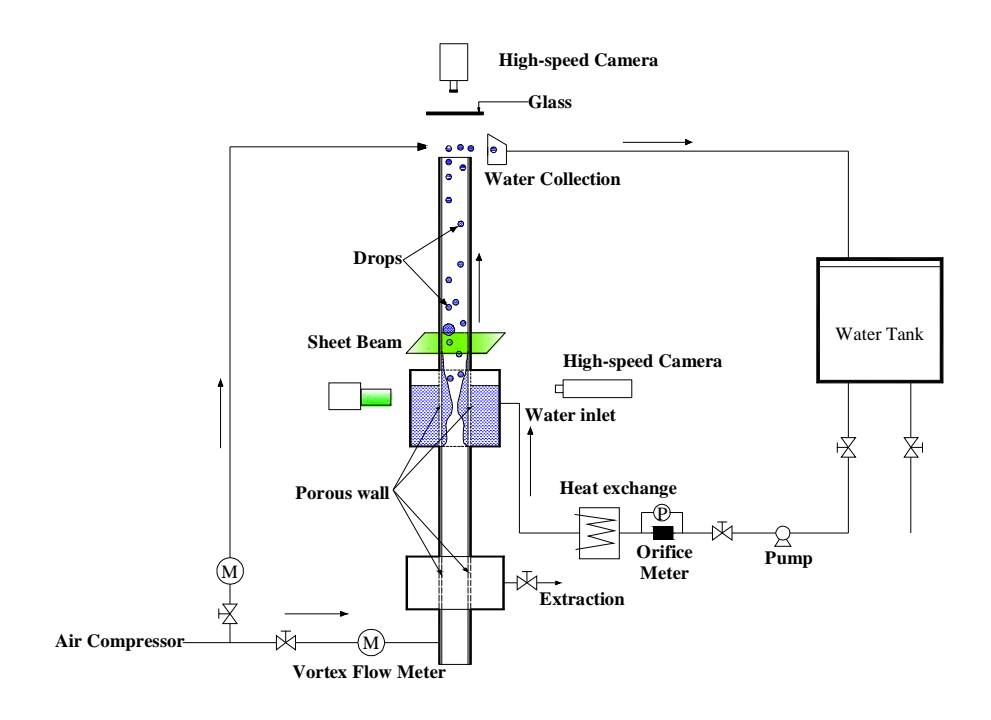


Figure 1 Schematic of the test facility.

The test section is comprised of a plastic tube with holes, water inlet chamber and water extraction sinter. The plastic tube, made of transparent polymethyl methacrylate, is 2m long and the inner diameter is 19mm. The water inlet section was arranged with 300 holes in 1mm diameter staggered in 15 rows and the holes spacing is about 2mm. Obviously, the configuration of the air-water mixer has an important influence on wave formation. In order to achieve circumferentially uniform distribution of liquid phase as in Taylor bubble, water flows into the test section has to be smooth and well-distributed. This was achieved by making the holes small and uniform-distributed. Moreover, the water extraction section consists of 250 holes with 1mm diameter. Inevitably, small amount of gas may be extracted with a falling liquid film from the water extraction sinter. A valve was introduced to control the amount of gas leaving from the extraction sinter. Therefore the amount of extracted gas is negligible. The air is metered by a rotor flow meter whilst water is metered by a deferential pressure transducer connected to an orifice flow meter. In addition, the upward liquid mass flux is measured by weighing method.

Two Memrecam fx K3 high-speed CCD cameras, which could run up to 10000 frame/s, were used for the flow visualization. In the present work, the sample frequency was set to 100 frame/s. The cameras were placed on the opposite side of the tube from backlight and at the outlet of the tube, respectively. In addition, a sheet beam and a backlight illumination were employed to illuminate the cross-section of the tube and the water inlet section, respectively. In order to prevent the gas-drop mixture interfere the work of CCD positioned at the outlet of the test section, a strong lateral direction wind was introduced to avoid the injected liquid, which gives a good protection of CCD lens from being polluted.

2.2 Experimental Procedure

In the present paper the experimental method of Barbosa et al. [17] was adopted. The gas flow was firstly introduced into the test section at a lower value and then the liquid flowed into the water inlet chamber at a constant value. Under these circumstances, liquid was injected through an inlet sinter and flowed downwards as a falling film and removed from the test section through the outlet sinter. Then, the gas flow rate was increased until liquid film ceased near the outlet sinter and then to the desire value. Waves were observed repeatedly formed in the region of the water inlet and transported upwards into the upper part of the tube. In the process of moving upwards, the flooding waves broke up into drops, which made the upper flow very oscillating. Thus, there are essentially two regions, one above the injector which is in churn flow and one below the injector which is of falling film flow with a counter- current gas flow.

All the experiments have been carried out near atmospheric pressure and a range of flow conditions were investigated. The water temperature is about 293K. Data were collected for predetermined gas and liquid flow conditions and for gas volume flow ranging from 5.0 to 13.0 m³/h and liquid mass flow ranging from 16.29e-3 to 40.89e-3 kg/s. The experimental conditions are plotted on the flow pattern map of Hewitt and Roberts [19] in Figure 2, respectively. It can be observed that all the experiments are performed under a churn or churn/annular flow condition.

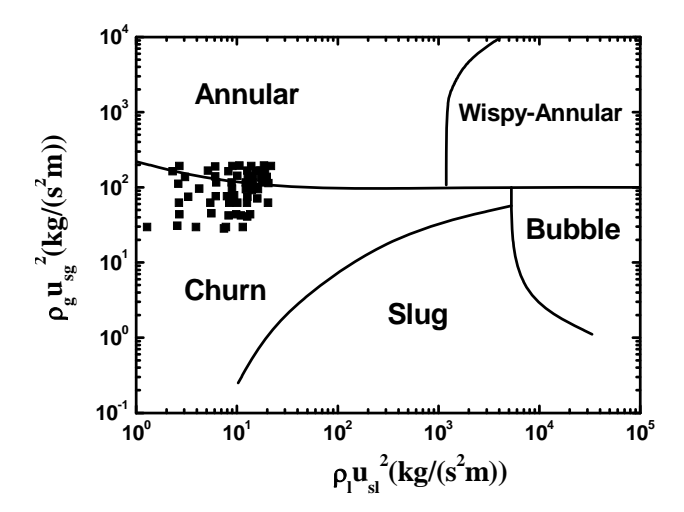


Figure 2 Flow pattern map of Hewitt and Roberts [19].

3. Results and discussions

3.1 Visualization of flooding waves in churn flow

Figures 3(a)-(d) depict the entire entrainment process in churn flow and demonstrate how the evolution of an individual flooding wave eventually leads to liquid entrainment. It is assumed that an individual wave has already generated in the water inlet section at t=0 ms, as seen in Figure3 (a). Figure 3(b) shows that the wave grows in both the radial and axial directions and moves slightly down the porous section. At t=30ms, the wave crest almost reaches its critical amplitude or even forms liquid bridge at this circumstance. In the next process of evolving, the wave which takes liquid from a falling film due to gravity above them starts to travel upwards, as seen in Figure 3(c). Eventually, the wave was tore by the higher-speed gas phase and entrained into the gas core. It also can be observed that the upper liquid film seems oscillating in the flow direction. At t=80 ms the wave has almost passed through the top of the frame, and another new wave is starting to form at the inlet section. This seems to be good circumstantial evidence that the breakdown of slug flow and the initiation of churn flow occur due to the onset of flooding waves in the Taylor bubble region of the slug flow.

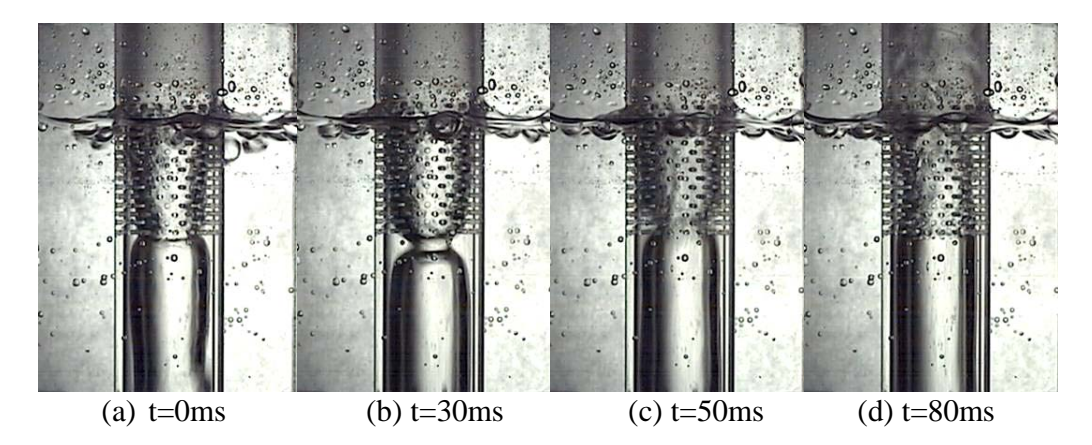


Figure 3 Evolution of flooding waves in churn flow. $(u_{sg}=6.17\text{m/s}, u_{sl}=74.85\text{e}-2\text{m/s}, U^*=0.49)$

Due to the gravity, it can be seen above that the flooding wave would firstly move downwards for a distance till a "balanced" position and finally be reversed to move upwards. Figures 4 (a)-(d) show the positions where flooding waves were reversed to travel upwards under different gas flow rate with constant total liquid mass flow rate G_l . The results indicate that the smaller the superficial gas velocity, the longer distance that waves travel downward. After collapse of the flooding waves, the liquid film performs quite differently at different flow conditions, as seen in Figures 5(a)-(e). The results imply that at the same total liquid flow rate, the liquid film becomes much distorted at lower superficial gas velocity because of the insufficient shear stress. In addition, the sickness of liquid film downward becomes thinner as gas flow rate increases, and finally disappears in annular flow.

The 14th International Topical Meeting on Nuclear Reactor Thermalhydraulics, NURETH-14 Toronto, Ontario, Canada, September 25-30, 2011

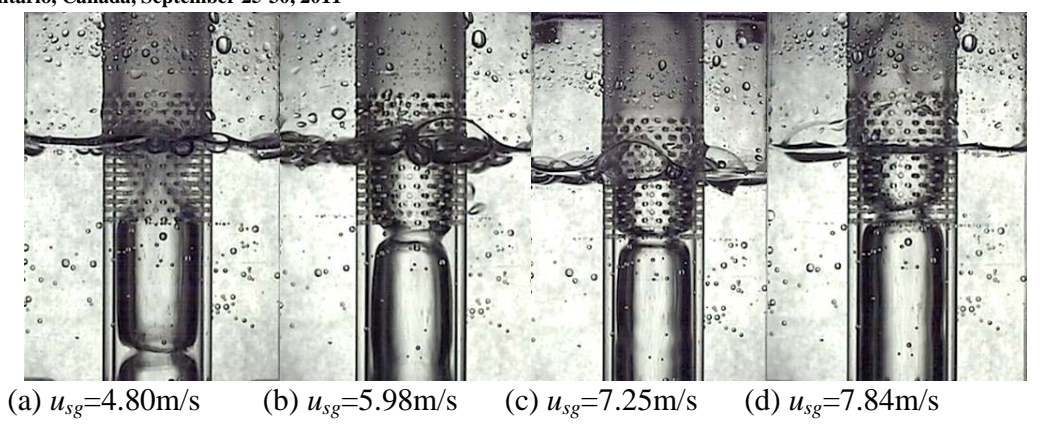


Figure 4 The positions where flooding waves were reversed to travel upwards at different superficial gas velocity (G_l =16.25e-2kg/s).

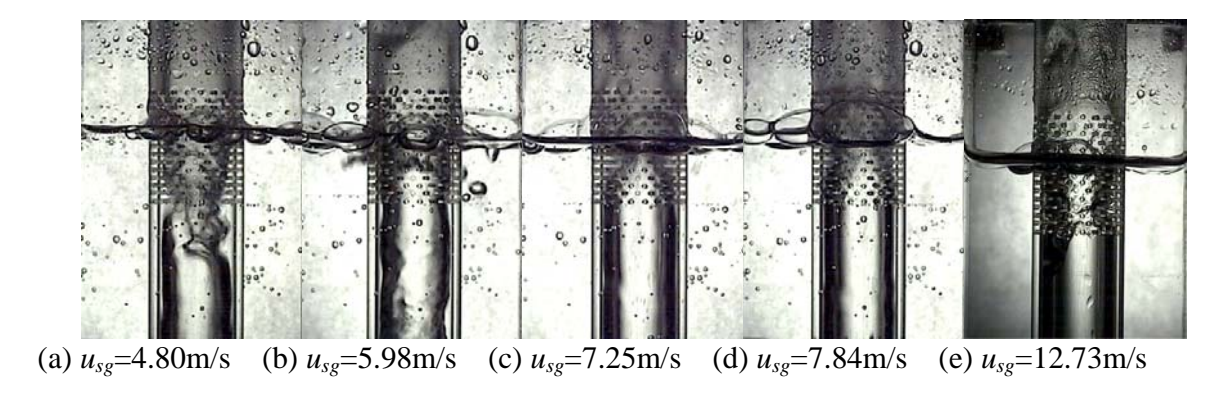
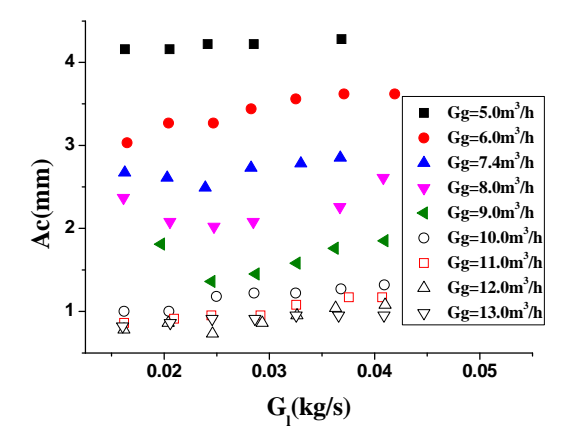


Figure 5 Comparison of oscillation at different flow conditions (G_l =16.25e-2kg/s).

From the observation, the wave forming at the liquid inlet continues growing until it reaches a critical amplitude big enough that it can be carried upwards. The critical amplitude of interfacial wave Ac varies under different gas and total liquid flow rate is shown in Figure 6. The results indicate that liquid mass flow rate has little impact on critical amplitude, and the critical amplitude decreases with the increase in gas flow rate. Beyond the reversal point, the wave amplitude continues growing to maximum amplitude Amax until the mass flow rate leave out of wave and entrained mass flow rate balance the mass flow rate inlet the wave. Figure 7 shows the maxima amplitude of interfacial wave varies under different gas and total liquid flow rate. Different from critical amplitude, the maximum amplitude decreases with the increasing of gas mass flux but increase with the increasing of liquid mass flux.



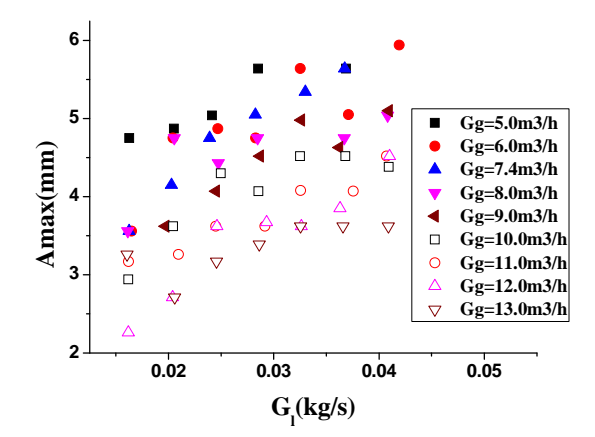
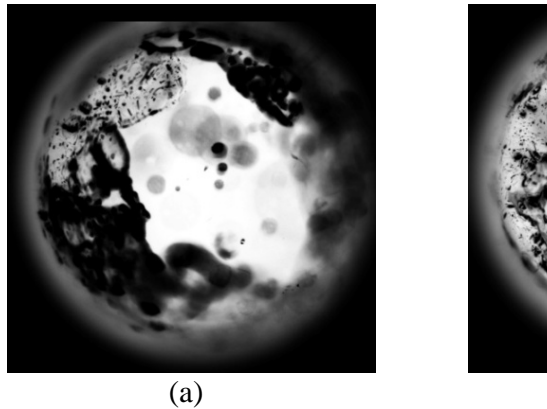


Figure 6 Critical amplitude of interfacial waves at different flow conditions

Figure 7 Maximum amplitude of interfacial waves at different flow conditions

For annular flow in a small-diameter tube, the liquid film is uniformly distributed around the tube circumference and disturbance waves appear circumferentially coherent. Therefore, annular flow is usually treated as two-dimensional and circumferentially symmetrical (Hewitt and Hall-Taylor [4]; Ohba and Nagae [20]). The liquid distribution of churn flow in the cross-section of tube is shown in Figure 8. It can be observed that the circumferential distribution of liquid film is non-uniform, which is quite different from that in annular flow. We suppose that the oscillations in liquid film lead to this irregular distribution. Therefore, 2D simplification may not be appropriate in the simulation under churn flow condition because of the lack in describing the real characteristics of this special flow pattern.



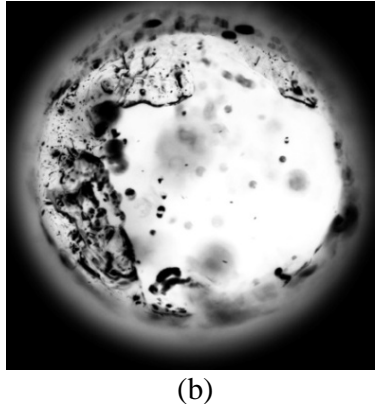


Figure 8 Axial view of churn flow.

3.2 Frequency of flooding waves

As mentioned before, waves transport liquid upwards whilst the base film between them flows downwards under gravity. The net liquid mass flow rate G_{nl} (the liquid that waves carried upward) may varies from 0 to total liquid mass flow rate when superficial gas velocity increases from churn flow to annular flow condition. Part of experiment data are list in Table 2.

The 14th International Topical Meeting on Nuclear Reactor Thermalhydraulics, NURETH-14 Toronto, Ontario, Canada, September 25-30, 2011

Table2. Data bank of various experiments in different conditions

V_g (m ³ /h)	$G_l \times 10^{-3}$	$G_{nl} \times 10^{-3}$	u_{sg}	$u_{sl} \times 10^{-3}$	U^*	P _o	f_{\cdot}
(m^3/h)	(kg/s)	(kg/s)	(m/s)	(m/s)	U	Re_g	(s^{-1})
5.1	20.51	10.15	5.00	35.90	0.40	6079.04	8.36
5.1	28.52	17.74	5.00	62.75	0.40	6079.04	8.77
5.1	36.86	24.98	5.00	88.36	0.40	6079.04	8.79
6.2	20.43	14.66	6.07	51.86	0.49	7390.21	8.71
6.1	28.28	25.78	5.98	91.19	0.48	7271.01	10.50
6.1	37.09	29.63	5.98	104.81	0.48	7271.01	11.17
7.4	20.29	14.61	7.25	51.68	0.58	8820.57	11.02
7.4	28.25	25.95	7.25	91.80	0.58	8820.57	12.96
7.4	36.75	31.80	7.25	112.49	0.58	8820.57	13.24
8.1	20.55	16.25	7.94	57.48	0.63	9654.95	11.95
8.2	28.47	25.26	8.03	89.36	0.64	9774.14	13.33
8.1	36.71	31.91	7.94	112.88	0.63	9654.95	13.33

Figure 9 shows the relationship between net liquid mass flow rate G_{nl} and total liquid mass flow rate G_{l} under different gas flow rates G_{g} . Obviously, net liquid mass flow rate increases with increase total liquid mass flow rate gas flow rate, and finally equals to total liquid mass flow rate gas flow rate in annular flow. Figure 10 shows net liquid mass flow rate carried by waves under different gas and total liquid flow rate. As expected, the net liquid mass flux increases with the increase in gas flow rate and total liquid flow flux. As the gas velocity increases, more liquid are brought upwards due to the increase of interfacial shear stress. On the other hand when the total liquid flow rate increases at a given gas velocity, the wave amplitude increases, which may also takes more liquid upwards.

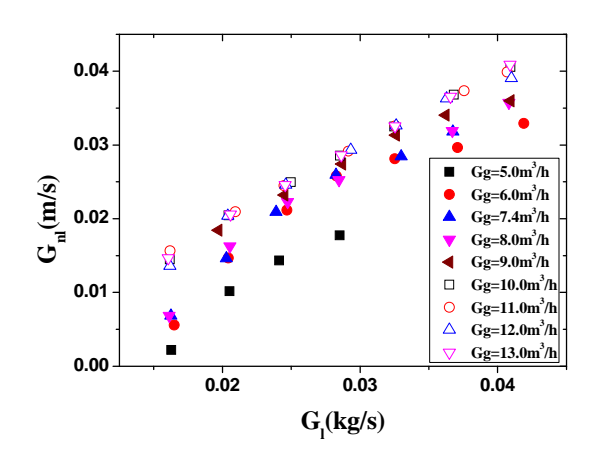


Figure 9 Relationship between net liquid mass flow rate and total liquid mass flow rate under different gas flow rates

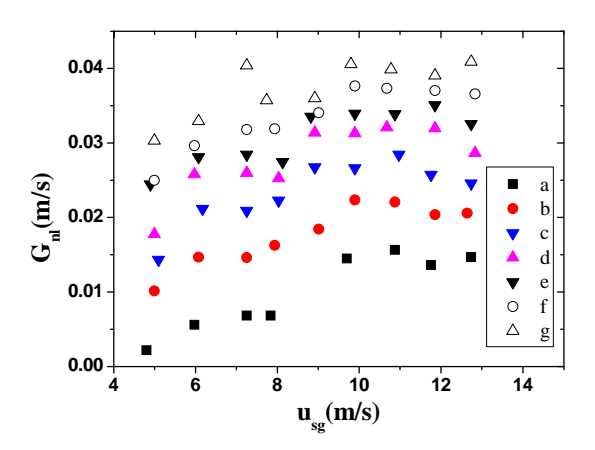


Figure 10 Comparison of the net liquid mass flow rates at different total liquid mass flow rates. (a=16.29E-3(kg/s), b=20.45E-3(kg/s), c=24.36E-3(kg/s), d=28.38E-3(kg/s),e=32.75E-3(kg/s), f=36.85E-3(kg/s), g=40.89E-3(kg/s))

Figure 11 shows the dependence of flooding wave frequency on gas superficial velocity and liquid superficial velocity. The result indicates that the wave frequency increases with increase of gas and liquid velocities. Also it appears that, at higher gas velocities, the wave frequency approximately approaches a constant value and shows very weak dependence on liquid velocity. It is because that the flooding wave reaches its maximum amplitude and eventually bursts more quickly at higher gas velocity before the liquid affects the frequency. In addition, wave frequency seems discontinuous change from churn flow to annular. Figure 12 shows the comparison of experiment results with Hewitt et al. [8] and Barbosa et al. [17]. The results are plotted against the gas Reynolds number Reg and the average cross section of net liquid mass flow rate $\overline{G}_{n'}(\times 10\text{-}3\text{kg/m2s})$. From the experiment data of present work, the wave frequency has a direct proportion with the gas Reynolds number and has little dependency on liquid mass flow rate. Due to the limited experiment data from Barbosa et al. [12], little conclusion can be further inferred. However, the experiment data from Hewitt et al. [8] are quite different. It can be observed that the range of wave frequency is much larger and the wave frequency has a strong dependency on liquid mass flow rate. The frequency increases with the increase in gas velocity at lower net liquid mass flow rate, but inverses at higher net liquid mass flow rate. Physical properties and pipe diameter are suspected to be the reason of this distinction. The experiment of Hewitt et al. was carried out in a 10mm vertical tube and the fluids are trichloroethylene and air. Moreover, near the same gas Reynolds number and the average cross section of net liquid mass flow rate, the wave frequency is higher in smaller diameter. It is supposed that gas velocity is much higher for smaller gas circulation area, which leads to higher wave frequency.

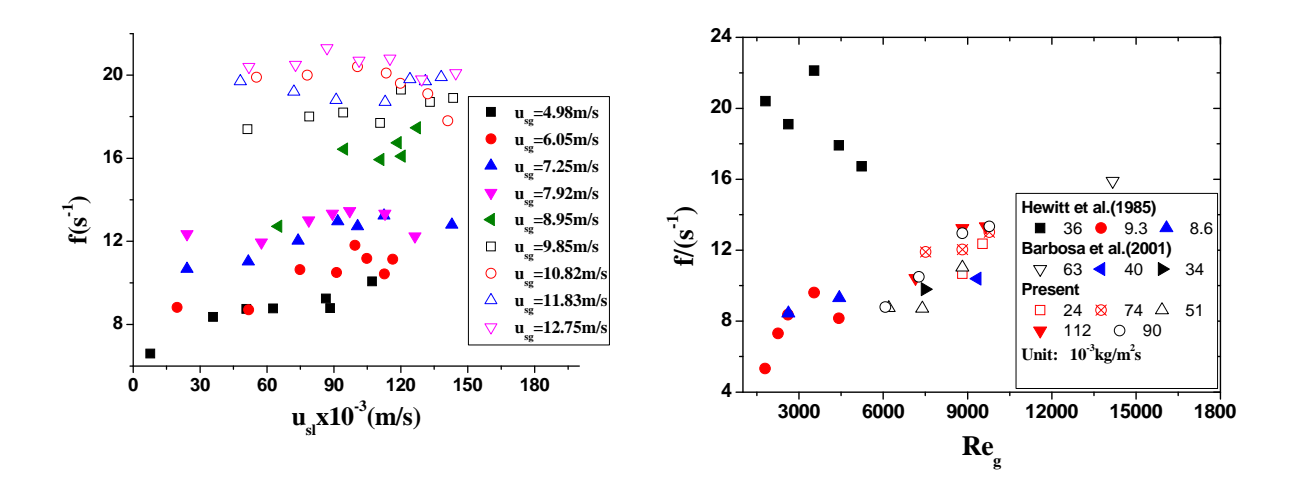


Figure 11 the frequency of flooding waves at different flow conditions.

Figure 12 Comparison of wave frequency with data of Hewitt et al. [8] and Barbosa et al. [17].

4. Conclusions

A good understanding of characteristics of flooding wave in churn flow is essential for the accurate prediction of CHF. High-speed visualization has been employed for qualitative investigation of the characteristics of churn flow. It was experimentally shown that flooding waves periodically appeared at the water inlet section and travelled upward and eventually entrained into the gas core. In addition, the liquid film was more instable at lower gas superficial velocity due to the insufficient

shear stress. The liquid distribution in the cross-section of pipe seems non-uniform, which demonstrated the drastic change in this flow regime. Moreover, the wave frequency increases with the increase in gas and liquid flow rate, but the amplitude is in contrary. Comparison of data with Hewitt et al. [8] and Barbosa et al. [17] shows a sensible difference, which can be attributed to the difference in fluid properties and pipe diameter.

5. References

- [1] M. Ahmad, et al., "Drop entrainment in churn flow", 7th International Conference on Multiphase Flow, Tampa, FL USA, 2010.
- [2] N. Zuber and J.A. Findlay, "Average volumetric concentration in two-phase flow systems", *Journal of Heat Transfer*, 1965, pp. 453-468.
- [3] Y. Taitel, D. Barnea, A.E. Dukler, "Modelling of flow pattern transitions for steady upward gas-liquid flow in vertical tubes". *A.l.Ch.E.J.*, Vol.26, 1980, pp. 345-354.
- [4] G.F. Hewitt and N. Hall-Taylor, "Annular two-phase flow", Pergamon Press, Oxford, 1970.
- [5] S. Jayanti and G. Hewitt, "Prediction of the slug-to-churn flow transition in vertical two-phase flow", *International journal of multiphase flow*, Vol. 18, No. 6, 1992, pp. 847-860.
- [6] S. Jayanti, G.F. Hewitt, D.E.F. Low, E. Hervieu, "Observation of flooding in the Taylor bubble of co-current upwards slug flow", *International journal of multiphase flow*, Vol. 19, No. 3, 1993, pp. 531-534.
- [7] D.G. Owen, "An experimental and theoretical analysis of equilibrium annular flows", Ph.D. Thesis, University of Birmingham, UK, 1986.
- [8] Hewitt, G.F., Martin, C.J., Wilkes, N.S., "Experimental and modelling studies of annular flow in the region between flow reversal and the pressure drop minimum". *PCH Physicochemical Hydrodynamics*, Vol.6,No.1/2,1985, pp.69-86.
- [9] Wallis, G.B., "One-Dimensional Two-Phase Flow". McGraw-Hill, New York, 1969.
- [10] P.H.J. Verbeek, R. Miesen and C.J. Schellenkens, "Liquid entrainment in annular dispersed upflow", <u>8th Annual European Conference on Liquid Atomization and Spray Systems</u>, Amsterdam, 30 September-2 October, 1992, pp. 33-45.
- [11]B.J. Azzopardi and S.H. Zaidi, "Determination of entrained fraction in vertical annular gas/liquid flow", *Journal of fluids engineering*, Vol. 122, 2000, pp, 146-150.
- [12] J.R. Barbosa, G.F. Hewitt, G. König and S.M. Richardson, "Liquid entrainment, droplet concentration and pressure gradient at the onset of annular flow in a vertical pipe", *International journal of multiphase flow*, Vol. 28, No. 6, 2002, pp. 943-961.
- [13] Wallis, G.B., The onset of droplet entrainment in annular gas-liquid flows. General Electric Report, No. 62GL127, 1962.
- [14] B.J. Azzopardi and E. Wren, "What is entrainment in vertical two-phase churn flow"? *International journal of multiphase flow*, Vol. 30, No. 1, 2004, pp. 89-103.
- [15] B.J. Azzopardi, "Drops in annular two-phase flow", *International journal of multiphase flow*, Vol. 23, 1997, pp. 1-53.

The 14th International Topical Meeting on Nuclear Reactor Thermalhydraulics, NURETH-14 Toronto, Ontario, Canada, September 25-30, 2011

- [16] A.H. Govan, G.F. Hewitt, H.J. Richter and A. Scott, "Flooding and churn flow in vertical pipes", *International journal of multiphase flow*, Vol. 17, 1991, pp. 27-44.
- [17] J. Barbosa, A.H. Govan and G.F. Hewitt, "Visualization and modelling studies of churn flow in a vertical pipe", *International journal of multiphase flow*, Vol. 27, No. 12, 2001, pp. 2105-2127.
- [18] E. Da Riva and D. Del Col, "Numerical simulation of churn flow in a vertical pipe", *Chemical Engineering Science*, Vol. 64, No. 17, 2009, pp. 3753-3765.
- [19] G.F. Hewitt and D. Roberts, "Studies of two-phase flow patterns by simultaneous X-ray and flash photography", <u>Atomic Energy Research Establishment</u>, Harwell (England), 1969.
- [20] K. Ohba, and K. Nagae, "Characteristics and Behaviour of the Interfacial Wave on the Liquid Film in a Vertically Upward Air-Water Two-Phase Annular Flow", *Nuclear Engineering and Design*, Vol. 141, No. 1-2, 1993, pp. 17-25.